

International Journal of Modern Physics E
 © World Scientific Publishing Company

SELF-CONSISTENT DESCRIPTION OF COLLECTIVE EXCITATIONS IN THE UNITARY CORRELATION OPERATOR METHOD

N. PAAR*† P. PAKONSTANTINO, R. ROTH, AND H. HERGERT

*Institut für Kernphysik, Technische Universität Darmstadt,
 Schlossgartenstrasse 9, D-64289 Darmstadt, Germany*

Received (received date)
 Revised (revised date)

The fully self-consistent Random Phase Approximation (RPA) is constructed within the Unitary Correlation Operator Method (UCOM), which describes the dominant interaction-induced short-range central and tensor correlations by a unitary transformation. Based on the correlated Argonne V18 interaction, the RPA is employed in studies of multipole response in closed-shell nuclei across the nuclide chart. The UCOM-RPA results in a collective character of giant resonances, and it describes rather well the properties of isoscalar giant monopole resonances. However, the excitation energies of isovector giant dipole resonances and isoscalar giant quadrupole resonances are overestimated due to the missing long-range correlations and three-body contributions.

1. Introduction

One of the unresolved problems in the theory of nuclear structure is the description of ground state properties and excitation phenomena for heavier nuclei, based on realistic nucleon-nucleon (NN) interactions which reproduce the NN scattering data ^{1,2,3}. The use of these realistic interactions for solving the nuclear many-body problem is a challenging task. Presently, only light nuclei can be treated within ab initio schemes like Green's function Monte Carlo ⁴, no-core shell model ⁵, and coupled cluster method ⁶. The Unitary Correlation Operator Method (UCOM), which describes the dominant short-range and tensor correlations explicitly by means of a unitary transformation ^{7,8,9,10}, allows for the use of realistic NN interactions in traditional nuclear structure methods. In contrast to other methods using unitary transformations, e.g. the unitary model operator approach ^{11,12}, the correlation operators are given explicitly allowing for the derivation of a system-independent effective interaction operator V_{UCOM} . Although different by its construction, the correlated NN interaction V_{UCOM} is similar to the V_{low-k} low-momentum interac-

*on leave of absence from Physics Department, Faculty of Science, University of Zagreb, Croatia

†corresponding author: nils.paar@physik.tu-darmstadt.de

2 *N. Paar, P. Papakonstantinou, R. Roth, and H. Hergert*

tion¹³. Both approaches lead to the separation of momentum scales, providing a phase-shift equivalent NN interaction in the low-momentum regime.

Very recently, the correlated realistic NN interaction constructed within the UCOM framework, has been employed in Hartree-Fock (HF) calculations across the nuclide chart¹⁴. Based on the UCOM-HF ground state, we have constructed the random-phase approximation (RPA) for the description of low-amplitude collective excitations in atomic nuclei using correlated realistic NN interactions¹⁵. Various phenomenological RPA and quasiparticle RPA models have been very successful in the past, not only in studies of giant resonances and low-lying states (e.g. Refs.^{17,18,19,20,21}), but also in description of exotic nuclear structure of collective excitations in nuclei away from the valley of β -stability^{20,22,23,24,25,26,27,28}. The present study, however, provides the first insight into the collective excitation phenomena in closed-shell nuclear systems, based on the correlated realistic NN interactions.

2. Unitary Correlation Operator Method (UCOM)

The essential ingredient of the UCOM approach is the explicit treatment of the interaction-induced correlations, i.e. short-range central and tensor correlations^{7,8,9}. The relevant correlations are imprinted into an uncorrelated many-body state $|\Psi\rangle$ through a state-independent unitary transformation defined by the unitary operator C , resulting in a correlated state $|\tilde{\Psi}\rangle = C|\Psi\rangle$. An equivalent, technically more advantageous approach, is based on using the correlated operators $\tilde{O} = C^\dagger O C$ with uncorrelated many-body states. The short-range central correlations are described by a distance-dependent shift, pushing two nucleons apart from each other if they are closer than the core distance. The application of the correlation operator in two-body space corresponds to a norm conserving coordinate transformation with respect to the relative coordinate. This transformation is parameterized in terms of correlation functions for each (S, T) channel which are determined by an energy minimization in the two-body system. For purely repulsive channels an additional constraint on the range of the central correlator is used ($I_{R_+}^{(S=0, T=0)} = 0.1 \text{ fm}^4$, cf. Ref.¹⁰). The details of the determination and parameterization of the standard correlator are given in Ref.¹⁰. The tensor correlations between two nucleons are generated by a tangential shift depending on the spin orientation⁸. The size and the radial dependence is given by a tensor correlation function $\vartheta(r)$ for each of the two $S = 1$ channels, whose parameters are also determined from an energy minimization in the two-body system¹⁰. The range of the tensor correlation function is restricted through a constraint on the range measure $I_\vartheta = \int dr r^2 \vartheta(r)$. If one would use for the description of finite nuclei the long-range tensor correlator that is optimal for the deuteron, an effective screening due to other nucleons would emerge through higher-order contributions of the cluster expansion⁸. In practical calculations based on two-body approximation, this problem is resolved by restricting the range of the tensor correlation function, which

provides an effective inclusion of the screening effect without explicit evaluation of higher terms in the cluster expansion⁹. Recent studies within the exact no-core shell model¹⁰, show that $I_{\varrho}^{(S=1,T=0)} = 0.09 \text{ fm}^3$ leads to an optimal tensor correlator for the description of binding energies of ${}^3\text{H}$ and ${}^4\text{He}$. In the present work we vary the range of the tensor correlator, $I_{\varrho}^{(S=1,T=0)} = 0.07, 0.08, \text{ and } 0.09 \text{ fm}^3$, in order to probe its impact on the description of the global properties of collective excitation phenomena in atomic nuclei. The contributions of the tensor correlator in $(S, T) = (1, 1)$ channel are one order of magnitude smaller⁹, and therefore neglected in the present study.

3. Random-phase approximation in the UCOM framework

Starting from the uncorrelated Hamiltonian for the A -body system consisting of the kinetic energy operator T and a two-body potential V , the formalism of the unitary correlation operator method is employed to generate the correlated Hamiltonian. By combining the central and tensor correlation operators, the correlated many-body Hamiltonian in two-body approximation is given by,

$$H_{\text{UCOM}} = \tilde{T}^{[1]} + \tilde{T}^{[2]} + \tilde{V}^{[2]} = T + V_{\text{UCOM}}, \quad (1)$$

where the one-body contribution comes only from the uncorrelated kinetic energy $\tilde{T}^{[1]} = T$. Two-body contributions arise from the correlated kinetic energy $\tilde{T}^{[2]}$ and the correlated potential $\tilde{V}^{[2]}$, which together constitute the correlated interaction V_{UCOM} ¹⁰. More details about the evaluation of the two-body matrix elements for V_{UCOM} are available in Ref.¹⁰. Assuming spherical symmetry, the correlated realistic NN interaction is employed to solve the HF equations, i.e. to evaluate the single-particle wave functions and energies¹⁴. The UCOM-HF single-particle spectra are used as a basis for the construction of the $p - h$ configuration space for the RPA. The RPA equations are derived from the equation of motion method using the quasiboson approximation¹⁷,

$$\begin{pmatrix} A^J & B^J \\ B^{*J} & A^{*J} \end{pmatrix} \begin{pmatrix} X^{\nu, JM} \\ Y^{\nu, JM} \end{pmatrix} = \omega_{\nu} \begin{pmatrix} 1 & 0 \\ 0 & -1 \end{pmatrix} \begin{pmatrix} X^{\nu, JM} \\ Y^{\nu, JM} \end{pmatrix}, \quad (2)$$

where the eigenvalues ω_{ν} correspond to RPA excitation energies. The residual particle-hole interaction in A and B matrices includes the correlated realistic NN interaction V_{UCOM} in a fully consistent way with the Hartree-Fock equations. In addition, the multipole transition operators are consistently transformed by employing the same unitary transformation as for the Hamiltonian.

However, it turns out that the effect of the UCOM transformation of the transition operators for monopole and quadrupole modes is negligible¹⁵. It is interesting to note, that the UCOM-RPA results are in agreement with the study of effective operators in the no-core shell model within the $2\hbar\Omega$ model space, where the B(E2) values are very similar for the bare and the effective operator which includes the two-body contributions¹⁶. An essential property of the present UCOM-RPA scheme

4 *N. Paar, P. Papakonstantinou, R. Roth, and H. Hergert*

is that it is fully self-consistent, i.e. the same correlated realistic NN interaction is used in the HF equations that determine the single-particle basis, as well as the RPA residual interaction, and the multipole transition operators are transformed consistently with V_{UCOM} . This means that the same unitary transformation of the realistic NN interaction, i.e. central and tensor correlation functions with the same set of parameters are systematically employed in HF and RPA calculations. The effective NN interaction which determines the ground-state properties, also determines the small amplitude motion around the nuclear ground state. This property of the present model ensures that RPA amplitudes do not contain spurious components associated with the center-of-mass translational motion. Models that are not fully self-consistent necessitate the inclusion of an additional free parameter in the residual interaction, to adjust a proper separation of the spurious state.

One of the interesting questions is to which extent the UCOM-RPA transition spectra are sensitive to the range of the tensor correlator employed in the unitary transformation. We have verified that the multipole strength distributions do not depend on variations of the central correlator range, around the standard short-range correlator¹⁵.

In Fig. 1, we display the UCOM-RPA spectra of isoscalar giant monopole resonances (ISGMR) for several closed-shell nuclei, using the correlated Argonne V18 interaction with different constrains on the range of the tensor correlator, $I_{\vartheta}^{(S=1,T=0)}=0.07, 0.08, \text{ and } 0.09 \text{ fm}^3$. For comparison, we also denote excitation energies from a selection of experimental^{29,30,31} and theoretical^{24,32,33} studies. The agreement with experiment and other theoretical results is rather good for the standard correlator set with $I_{\vartheta}^{(S=1,T=0)}=0.09 \text{ fm}^3$. In heavy nuclei, the ISGMR energies are overestimated by $\approx 1 - 3 \text{ MeV}$. By varying the range of the tensor correlator around its standard value, the transition strength can be fine-tuned to improve the agreement with the experimental data.

Next we employ the UCOM-RPA to describe the isovector giant dipole resonances (IVGDR) in ^{90}Zr , ^{132}Sn , and ^{208}Pb (Fig. 2). The correlated Argonne V18 interaction is used, with different constraints on the ranges of the tensor part of the correlator, $I_{\vartheta}^{(S=1,T=0)}=0.07, 0.08, \text{ and } 0.09 \text{ fm}^3$. The calculated dipole response is compared with the experimental data^{34,35,36,37} and with the theoretical excitation energies from the relativistic RPA³⁸ based on DD-ME2 interaction³⁹. In all nuclei under consideration, the resulting IVGDR strength distributions display rather wide resonance-like structures. The decrease in the range of the tensor correlator, i.e. its constraint $I_{\vartheta}^{(S=1,T=0)}=0.09 \text{ fm}^3$ towards 0.07 fm^3 , results in lower IVGDR peak energies by $\approx 2\text{-}3 \text{ MeV}$. However, UCOM-RPA overestimates the IVGDR centroid energies by $\approx 3\text{-}7 \text{ MeV}$. This difference can serve as a direct measure of the missing correlations and three-body contributions in the UCOM-RPA scheme. Inclusion of the three-body interaction and long-range correlations beyond the simple RPA method, would probably to a large extent resolve the presently obtained discrepancies with the other studies.

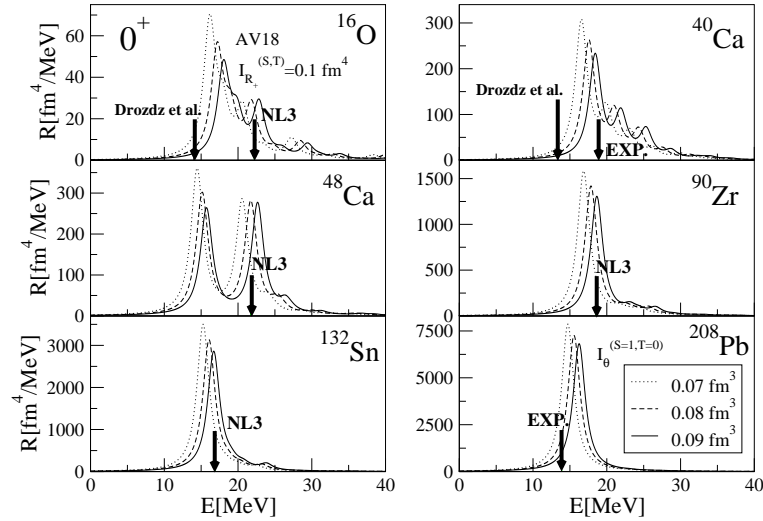


Fig. 1. The calculated UCOM-RPA strength distribution of ISGMR for the correlated Argonne V18 interaction, using different restrictions on the range of the tensor correlator ($I_{\vartheta}^{(S=1,T=0)}=0.07, 0.08, \text{ and } 0.09 \text{ fm}^3$). The experimental data^{29,30,31} and results from the nonrelativistic (Drożdż et al.)³² and relativistic RPA (NL3)^{24,33} are denoted by arrows.

In Fig. 3 we show the UCOM-RPA isoscalar quadrupole transition strength distributions for ^{40}Ca , ^{90}Zr , and ^{208}Pb (Argonne V18, $I_{\vartheta}^{(S=1,T=0)}=0.07, 0.08, \text{ and } 0.09 \text{ fm}^3$), in comparison with experimental data⁴⁰. The residual interaction constructed from the correlated realistic NN interaction is attractive in the isoscalar channel, generating strongly collective peaks corresponding to isoscalar giant quadrupole resonance (ISGQR). In addition, in the case of ^{90}Zr , and ^{208}Pb , the UCOM-RPA model also results with pronounced low-lying 2^+ states. However, RPA based on the correlated realistic NN interaction, without the long-range correlations and three-body contributions, is not sufficient for a quantitative description of ISGQR excitation energy. For the short range tensor correlator ($I_{\vartheta}^{(S=1,T=0)}=0.07 \text{ fm}^3$) the model still overestimates experimental values by $\approx 8 \text{ MeV}$. By decreasing the range of the tensor correlator, the quadrupole response is systematically shifted towards lower energies. The quadrupole response is rather sensitive to the range of the tensor correlator. For ^{40}Ca and the ranges of tensor correlator determined by $I_{\vartheta}^{(S=1,T=0)}=0.07, 0.08, \text{ and } 0.09 \text{ fm}^3$, the ISGQR centroid energies read 25.1, 26.2, and 27.1 MeV, respectively. In the cases of heavier nuclei, these differences are smaller, e.g. for ^{208}Pb , the centroid energy lowers by 1.2 MeV when going from the correlator with $I_{\vartheta}^{(S=1,T=0)}=0.09 \text{ fm}^3$ towards $I_{\vartheta}^{(S=1,T=0)}=0.07 \text{ fm}^3$.

The agreement achieved between the calculated and experimental properties of the ISGMR indicates that the correlated NN interaction corresponds to realis-

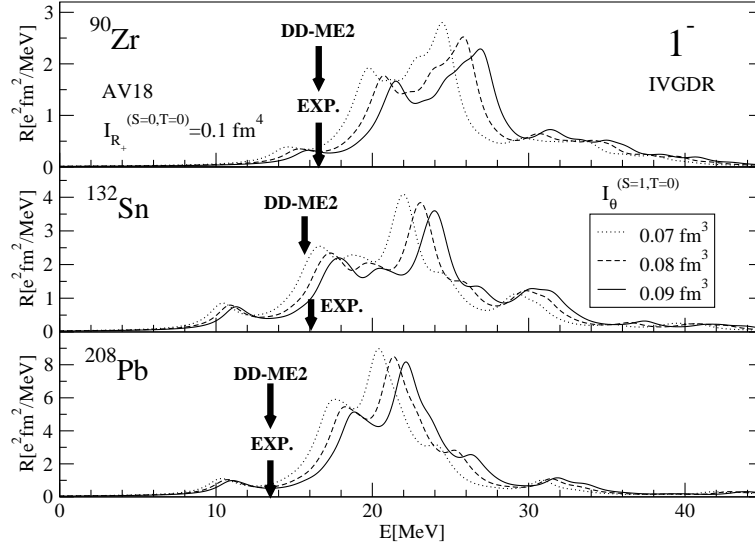
6 *N. Paar, P. Papakonstantinou, R. Roth, and H. Hergert*

Fig. 2. The UCOM-RPA strength distributions for the IVGDR in ^{90}Zr , ^{132}Sn , and ^{208}Pb . The calculations are based on the correlated Argonne V18 interaction, using different constraints on the tensor correlator range ($I_{\theta}^{(S=1, T=0)} = 0.07, 0.08, \text{ and } 0.09 \text{ fm}^3$). The experimental data ^{34,35,36,37} and the relativistic RPA (DD-ME2) energies ^{38,39} are shown by arrows.

tic values of the nuclear matter (NM) incompressibility. It has been demonstrated in the past that, within relativistic and non-relativistic RPA, the energies of the dipole and quadrupole resonances, on one hand, and the value of the effective mass corresponding to the effective interaction used, on the other, are correlated ^{41,42}. In particular, the relativistic RPA without density-dependent interaction terms, based on the ground state with a small effective mass and relatively high compression modulus, resulted in systematically overestimated energies of giant resonances ⁴¹. The discrepancies between UCOM-RPA calculations and experimental data for multipole giant resonances, as well as the low density of single-nucleon UCOM-HF states, suggest that the respective effective mass is too small. Tensor correlations with shorter range increase the single-particle level density and result in a systematic shift of the giant resonances towards lower energies, improving the agreement with experimental data. However, the variations of the ranges of correlation functions can serve only as a tool for fine tuning of the excitation spectra and they can not supplement the effects of the missing long-range correlations and three-body contributions.

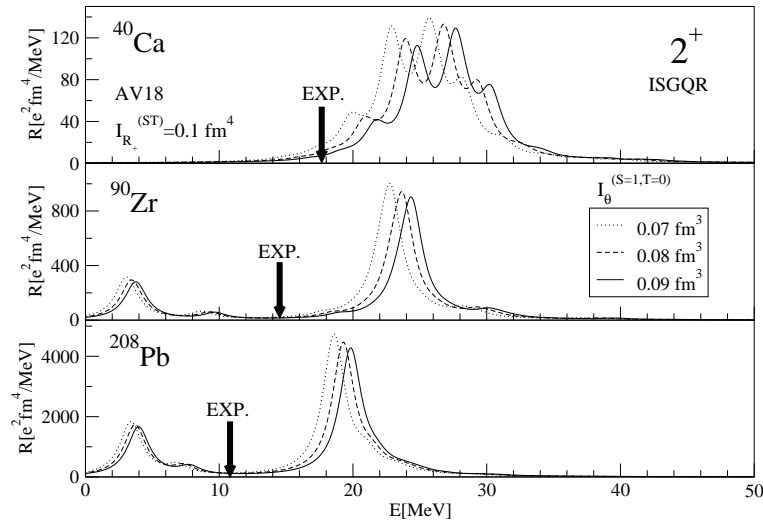


Fig. 3. The ISGQR strength distributions for ^{40}Ca , ^{90}Zr , and ^{208}Pb . The UCOM-RPA model is based on the correlated Argonne V18 interaction with different values of $I_{\theta}^{(S=1,T=0)} = 0.07, 0.08,$ and 0.09 fm^3 to constrain the range of the tensor correlator. The experimental ISGQR excitation energies are denoted by arrows ⁴⁰.

4. Conclusions

In the present study, the fully self-consistent RPA is formulated in the single-nucleon Hartree-Fock basis by using correlated realistic NN interactions. The short-range central and tensor correlations induced by the NN potential are explicitly treated within the UCOM framework. It is shown that the correlated NN interactions are successful in generating collective excitation modes, but for an accurate description of experimental data on excitation energies and transition strengths, one has to account for the contributions missing in the present treatment. These are (i) long-range correlations beyond simple RPA, which can be included within a RPA scheme built on the correlated ground state or by including complex configurations within Second-RPA, and (ii) induced and genuine three-body interactions, which one could try to model by a simple effective three-body force.

Acknowledgments

This work has been supported by the Deutsche Forschungsgemeinschaft (DFG) under contract SFB 634. We thank the Institute for Nuclear Theory at the University of Washington for its hospitality and the Department of Energy for partial support during the completion of this work.

8 *N. Paar, P. Papakonstantinou, R. Roth, and H. Hergert*

References

1. V. G. J. Stoks et al., *Phys. Rev.* **C49** (1994) 2950.
2. R. Machleidt, *Adv. Nucl. Phys.* **19** (1989) 189.
3. R. B. Wiringa, V. Stoks, and R. Schiavilla, *Phys. Rev.* **C51** (1995) 38.
4. S. C. Pieper, R. B. Wiringa, and J. Carlson, *Phys. Rev.* **C70** (2004) 054325.
5. P. Navrátil and W. E. Ormand, *Phys. Rev.* **C68** (2003) 034305.
6. M. Wloch, D. J. Dean, J. R. Gour, M. Hjorth-Jensen, K. Kowalski, T. Papenbrock, and P. Piecuch, *Phys. Rev. Lett.* **94** (2005) 212501.
7. H. Feldmeier, T. Neff, R. Roth, and J. Schnack, *Nucl. Phys.* **A632** (1998) 61.
8. T. Neff and H. Feldmeier, *Nucl. Phys.* **A713** (2003) 311.
9. R. Roth, T. Neff, H. Hergert, and H. Feldmeier, *Nucl. Phys.* **A745** (2004) 3.
10. R. Roth et al., *Phys. Rev.* **C72** (2005) 034002.
11. C. M. Shakin and Y. R. Waghmare, *Phys. Rev.* **161** (1967) 1006.
12. S. Fujii, R. Okamoto, and K. Suzuki, *Phys. Rev.* **C69** (2004) 034328.
13. S. K. Bogner, T. T. S. Kuo, A. Schwenk, *Phys. Rep.* **386** (2004) 1.
14. R. Roth et al., submitted to *Phys. Rev. C* (2005).
15. N. Paar et al., to be submitted to *Phys. Rev. C* (2005).
16. I. Stetcu, B. R. Barrett, P. Navrátil, and J. P. Vary, *Phys. Rev.* **C71** (2005) 044325.
17. D. J. Rowe, Nuclear Collective Motion - Models and Theory, Methuen and Co. LTD., London (1970).
18. T. S. Dumitrescu and F. E. Serr, *Phys. Rev.* **C27** (1983) 811.
19. John F. Dawson and R. J. Furnstahl, *Phys. Rev.* **C42** (1990) 2009.
20. I. Hamamoto, H. Sagawa and X. Z. Zhang, *Phys. Rev.* **C56** (1997) 3121.
21. G. Coló et al., *Phys. Lett.* **B485** (2000) 362.
22. M. Matsuo et al., *Phys. Rev.* **C71** (2005) 064326.
23. J. Terasaki et al., *Phys. Rev.* **C71** (2005) 034310.
24. N. Paar, P. Ring, T. Nikšić, and D. Vretenar, *Phys. Rev.* **C67** (2003) 034312.
25. D. Sarchi, P. F. Bortignon, and G. Coló, *Phys. Lett.* **B601** (2004) 27.
26. N. Paar, D. Vretenar, and P. Ring, *Phys. Rev. Lett.* **94** (2005) 182501.
27. P. Papakonstantinou et al., *Phys. Lett.* **B604** (2004) 157.
28. L. G. Cao and Z. Y. Ma, *Phys. Rev.* **C71** (2005) 034305.
29. D. H. Youngblood, H. L. Clark, and Y.-W. Lui, *Phys. Rev. Lett.* **82** (1999) 691.
30. S. Shlomo and D. H. Youngblood, *Phys. Rev.* **C47** (1993) 529.
31. M. M. Sharma and M. N. Harakeh, *Phys. Rev.* **C38** (1988) 2562.
32. S. Drożdż, S. Nishizaki, J. Speth, and J. Wambach, *Phys. Rep.* **197** (1990) 1.
33. Z. Y. Ma et al., *Nucl. Phys.* **A686** (2001) 173.
34. P. Adrich et al., *Phys. Rev. Lett.* **95** (2005) 132501.
35. B. L. Berman and S. C. Fultz, *Rev. Mod. Phys.* **47** (1975) 713.
36. T. D. Poelhekkens et al., *Phys. Rev. Lett.* **62** (1989) 16.
37. J. Ritman et al., *Phys. Rev. Lett.* **70** (1993) 533.
38. T. Nikšić, D. Vretenar, and P. Ring, *Phys. Rev.* **C66** (2002) 064302.
39. G. A. Lalazissis, T. Nikšić, D. Vretenar, and P. Ring, *Phys. Rev.* **C71** (2005) 024312.
40. F. E. Bertrand et al., *Phys. Lett.* **B80** (1979) 198.
41. M. L'Huillier and Nguyen Van Giai, *Phys. Rev.* **C39** (1989) 2022.
42. P.-G. Reinhard, *Nucl. Phys.* **A649** (1999) 305c.